Application of a Primitive Equation Barotropic Model to Predict Movement of "Western Disturbances"

Y. RAMANATHAN AND K. R. SAHA

Indian Institute of Tropical Meteorology, Poona-5, India

(Manuscript received 20 September 1971, in revised form 9 November 1971)

ABSTRACT

A primitive equation, limited-area, barotropic model with east-west cyclic boundary conditions is used to predict the movement of "Western Disturbances" in the Asian subtropics in two cases. Forecast and verification charts up to 72 hr and relevant error statistics are presented. Results are encouraging enough for the study of more such cases, and for the application of the model for low-latitude monsoon depressions and tropical cyclones.

1. Introduction

During the northern winter, a number of eastward moving baroclinic waves in the subtropical westerlies affect the northern parts of the Indian Subcontinent. In the course of their movement, some of these waves amplify and affect weather in the mountains and in the plains of northern India, while others simply move on without producing any appreciable change in prevailing weather. In India and neighboring countries, these disturbances are known as "Western Disturbances," since they move from the west and produce disturbed weather. Shukla *et al.* (1970) used a nondivergent barotropic model with streamfunctions derived from observed winds as input to forecast the movement of troughs in subtropical westerlies at 500 mb and found that the forecasts were fairly reasonable up to 24 hr but deteriorated beyond this period. In the present paper, the authors have applied a primitive equation barotropic model at 500 mb to predict the movement of western disturbances. A free-surface, divergent barotropic model which, in essence, conserves potential vorticity, is used for time integration. The model has been applied to two series of western disturbances during 1968 and 1969.

The following sections describe the model, finite-difference scheme, boundary conditions, data initialization, results and verification statistics. An indication of the further applications and experiments to be carried out with the model is given in the concluding section.

2. The model

The model equations in Cartesian coordinates on a Mercator projection are

$$\frac{\partial u}{\partial t}+m\left(u\frac{\partial u}{\partial x}+v\frac{\partial u}{\partial y}+g\frac{\partial h}{\partial x}\right)-fv=0, \quad (1)$$

$$\frac{\partial v}{\partial t}+m\left(u\frac{\partial v}{\partial x}+v\frac{\partial v}{\partial y}+g\frac{\partial h}{\partial y}\right)+fu=0, \quad (2)$$

$$\frac{\partial h}{\partial t}+m\left[u\frac{\partial h}{\partial x}+v\frac{\partial h}{\partial y}+h\left(\frac{\partial u}{\partial x}+\frac{\partial v}{\partial y}\right)\right]-vh\frac{\partial m}{\partial y}=0, \quad (3)$$

where u, v are the components of the wind vector along axes x, y pointing to east and north respectively, h is the height of the free surface at 500 mb, m a map factor (secant of latitude), f the Coriolis parameter, and t time.

3. Finite-difference scheme

The finite-difference analogue which Shuman called "semi-momentum" was adopted for space derivatives. For details, the reader is referred to Shuman (1962) and Shuman and Vandermann (1966). The time step used was 10 min. After the first forward-time step, a central-difference scheme was adopted. The grid interval used was 2.5° latitude-longitude intersections. Considering the scale of the disturbance and the data density in the subtropics, adoption of a grid size of 2.5° appears reasonable.

Gerrity and McPherson (1969) used a grid length of 190.5 km at 60N in their limited-area fine-mesh prediction model. Wang and Halpern (1970), who experimented with a regional fine-mesh grid superimposed upon a coarse hemispheric grid, also used a grid length of 190.5 km (true at 60N) for the fine mesh.

The mean height of the free surface at 500 mb was taken as 2.5 km. This choice involved the following considerations:

If H is the mean height of the 500 mb surface and ρ_2, ρ_1 are, respectively, the mean densities of the atmospheric columns above and below this surface, the speed

of the internal gravity wave, C_{gi}, is given by

$$C_{gi}=\pm[gH(1-\rho_2/\rho_1)]^{\frac{1}{2}}.$$

If the 500-mb surface is now assumed as a free surface with a mean height of H_1, then the speed of the external gravity wave, C_{ge}, is given by

$$C_{ge}=\pm(gH_1)^{\frac{1}{2}},$$

where $H_1=H(1-\rho_2/\rho_1)$. Since $H\approx 5.5$ km and $\rho_2/\rho_1 \approx 0.5$, a value of 2.5 km for H_1 was adopted.

4. Boundary conditions

Determining tractable boundary conditions for a restricted-area model traditionally poses a difficult problem. Gerrity and McPherson (1969) applied static boundary conditions throughout the forecast period. Wang and Halpern (1970) used two grid sizes, one coarse and the other fine, and the integration of the prediction equations over the fine-mesh utilized boundary values supplied by the coarse-mesh hemispheric model. In both the above-mentioned studies, height was used as initial data. The boundary conditions for the present study which uses winds as initial data are the following: A cyclic continuity is prescribed in the east-west direction to remove the need for east-west boundaries (Krishnamurti, 1969). This is achieved by introducing eight extra grid points in the zonal direction on the eastern side such that $A(1)=A(h+8)$ and $A(2)=A(h+7)$ where h is the number of grid points in the unextended mesh along the zonal direction and the A's represent data values. Data for the fictitious points are generated by a polynomial fit using values at grid points $h-1$, h, $h+7$ and $h+8$. With these boundary conditions it was anticipated that as far as slow-moving meteorological systems were concerned, the errors would be confined to the region in close proximity to the boundaries during the forecast period. This is further discussed in Section 7.

The north-south boundaries were treated as rigid walls to prevent any flow across the walls (Shuman and Vandermann, 1966). The equations at the boundaries are

$$\frac{\partial u}{\partial t}+m\left(u\frac{\partial u}{\partial x}+g\frac{\partial h}{\partial x}\right)=0, \tag{4}$$

$$v=0, \tag{5}$$

$$fu+mg\frac{\partial h}{\partial y}=0. \tag{6}$$

Eq. (4) was applied to the u tendency, Eq. (5) ensured a rigid boundary on the north and south walls when applied to the v field, and Eq. (6) maintained a geostrophic flow along the wall when imposed on the h field.

5. Data initialization

As already mentioned, the initial input to the model is derived from observed winds and not from height data. The choice in favor of winds was determined largely by the fact that the area of integration includes the tropical belt where wind data are known to be more plentiful and perhaps, more accurate, than height data. The initialization procedure involved computation of the nondivergent part of the wind and corresponding heights by solving a balance equation.

The nondivergent part of the wind, $\mathbf{V}_\psi$, is obtained from the solution of

$$\nabla^2\psi=m^2\left[\frac{\partial}{\partial x}\left(\frac{v}{m}\right)-\frac{\partial}{\partial y}\left(\frac{u}{m}\right)\right], \tag{7}$$

$$\mathbf{V}_\psi=\mathbf{k}\times\nabla\psi, \tag{8}$$

where ψ is the streamfunction. To solve (7) the boundary, n the distance along the normal to the boundary increasing outward and s the distance along the boundary. Integration of (9) around the boundary gives

$$\frac{\partial\psi}{\partial s}=-v_n+\frac{\partial\chi}{\partial n}, \tag{9}$$

where v_n is the velocity component normal to the boundary, n the distance along the normal to the boundary increasing outward and s the distance along the boundary. Integration of (9) around the boundary gives

$$\oint v_n ds=\oint\left(\frac{\partial\chi}{\partial n}\right)ds\equiv\overline{\frac{\partial\chi}{\partial n}}S, \tag{10}$$

where S is the total length of the boundary. We now replace (9) by (Hawkins and Rosenthal, 1965)

$$\frac{\partial\psi}{\partial s}=-v_n+\overline{\frac{\partial\chi}{\partial n}}. \tag{11}$$

With east-west cyclic continuity and v_n zero on the north-south boundaries, $\oint v_n ds$ and hence $\overline{\partial\chi}/\partial n$ is taken as zero and we use

$$\frac{\partial\psi}{\partial s}=-v_n \tag{12}$$

for obtaining the boundary values of ψ. Integrating along the boundary and assigning an arbitrary value of ψ at one of the grid points, the ψ values on the boundary were determined and Eq. (7) solved to get the ψ field; u_ψ and v_ψ were then obtained from (8).

The nondivergent terms u_ψ and v_ψ were used to calculate the forcing function on the right-hand side

of the balance equation for h given by

$$\nabla^2 h = \frac{1}{g}\frac{\partial}{\partial x}\left(u\frac{\partial u}{\partial x}+v\frac{\partial u}{\partial y}-\frac{fv}{m}\right)$$

$$\frac{1}{g}\frac{\partial}{\partial y}\left(u\frac{\partial v}{\partial x}+v\frac{\partial v}{\partial y}+\frac{fu}{m}\right). \quad (13)$$

As in Shuman and Vandermann (1966), the values on the right-hand side of (13) were normalized for two distinct sets of points to avoid the separation of solutions at alternate points resulting from the finite-difference equations. The boundary conditions in equations (5)–(6) were imposed during relaxation.

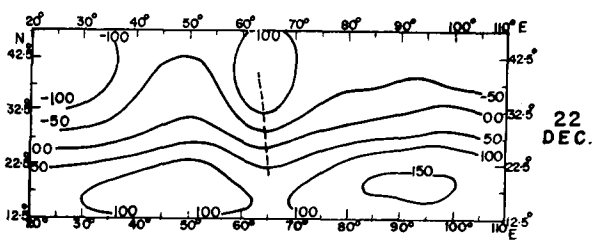

FIG. 1a. Initial map of first forecast series (0000 GMT 22 December 1968).

6. Data and results

The model was applied to two situations, one from 22–25 December 1968 and the other from 11–14 January 1969. The area of integration was 12.5–47.5N, 20–110E in the former case and 20–55N, 15–105E in the latter. The charts were hand-analyzed. The u, v components of the wind at 500 mb on 22 December 1968 and 11 January 1969 formed the initial data in the respective series.

Fig. 1 shows the initial chart and the 24-, 48- and 72-hr forecasts of the streamfunction field for the December 1968 case. Fig. 2 shows the corresponding charts for the 1969 case. The verifying streamfunction charts are shown on the right of the forecast charts in both figures. The charts do not include the extended portion of fictitious grid points used to remove the need for east-west boundaries.

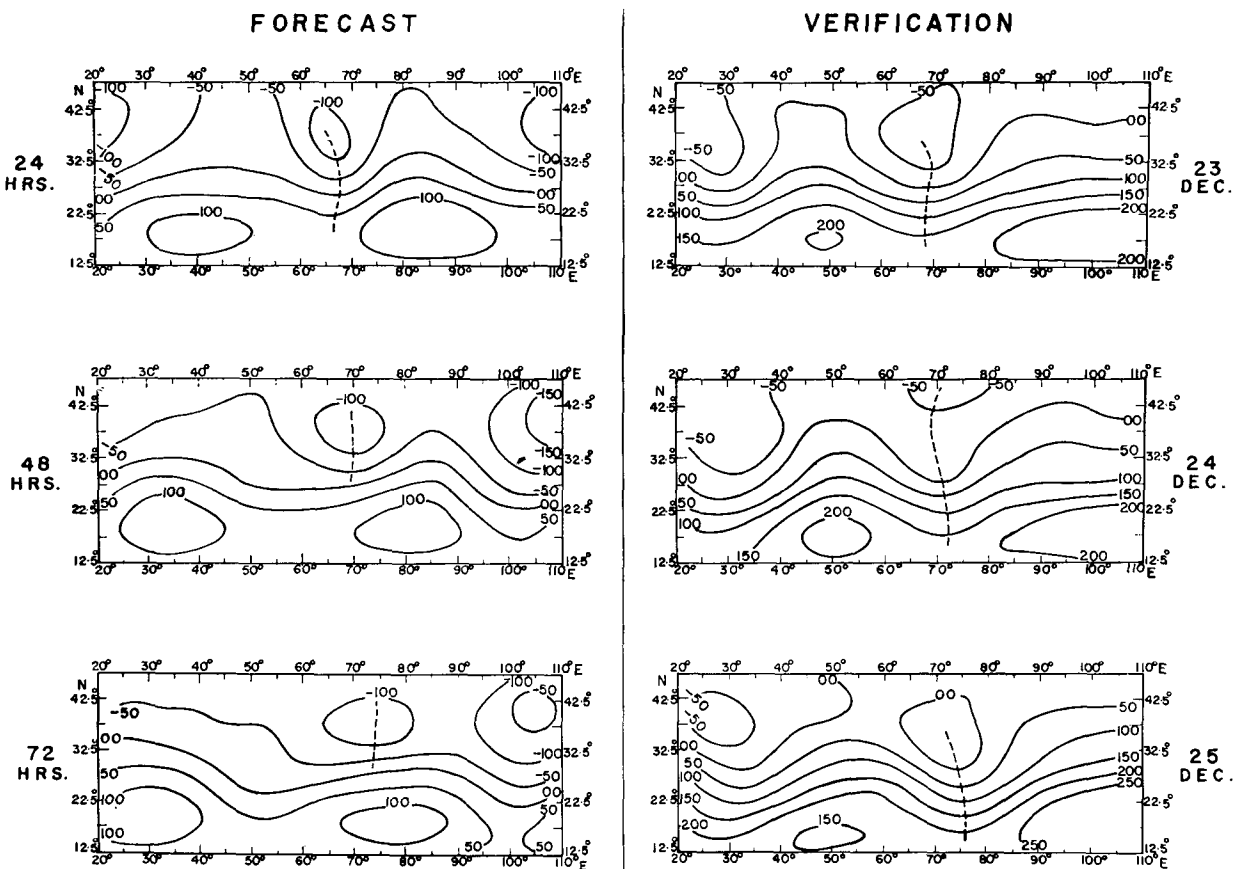

FIG. 1b. Forecast streamfunction charts at 500 mb for 24, 48 and 72 hr and corresponding verification streamfunction charts. Initial map is shown in Fig. 1a. The dashed line gives the position of the axis of the trough.

TABLE 1. Verification of forecasts of the u and v fields (m sec^{-1}).

Period of forecast (hr)	u component: Standard deviation of error	u component: Persistence error	u component: Correlation coefficient	v component: Standard deviation of error	v component: Persistence error	v component: Correlation coefficient
Initial chart 11 January 1969 (0000 GMT)						
24	4.4	6.6	0.6	5.1	7.0	0.6
48	5.7	7.0	0.6	7.3	7.8	0.6
72	7.5	7.7	0.6	7.8	8.2	0.5
Initial chart 22 December 1968 (0000 GMT)						
24	6.9	8.9	0.6	8.8	11.6	0.5
48	8.6	9.6	0.5	12.8	12.8	0.5
72	10.5	12.9	0.5	13.7	14.4	0.4

7. Verification statistics

Wang and Halpern (1970) have reported an rms error of 46.4 and 45.3 m for 24-hr height forecasts from their fine-mesh limited-area model, using balanced and non-balanced initial data, respectively. Since the present study uses wind as input and gives wind forecasts, it is difficult to compare our statistics with those involving height forecasts for limited-area models. Table 1 shows the results of verification of the forecasts computed separately for the u and v components. It gives the standard deviations of the forecast errors, errors of forecasts based on persistence, and the correlation coefficients between actual and forecast changes for the whole forecast domain.

The following general features appear to be revealed by Table 1:

1) Errors increase with period of forecast.
2) Errors in v-component forecasts are generally larger than those of u-component forecasts.

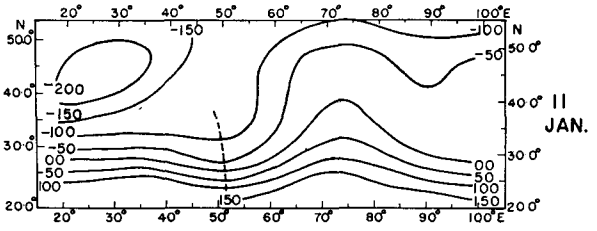

FIG. 2a. Initial map for second forecast series (0000 GMT 11 January 1969).

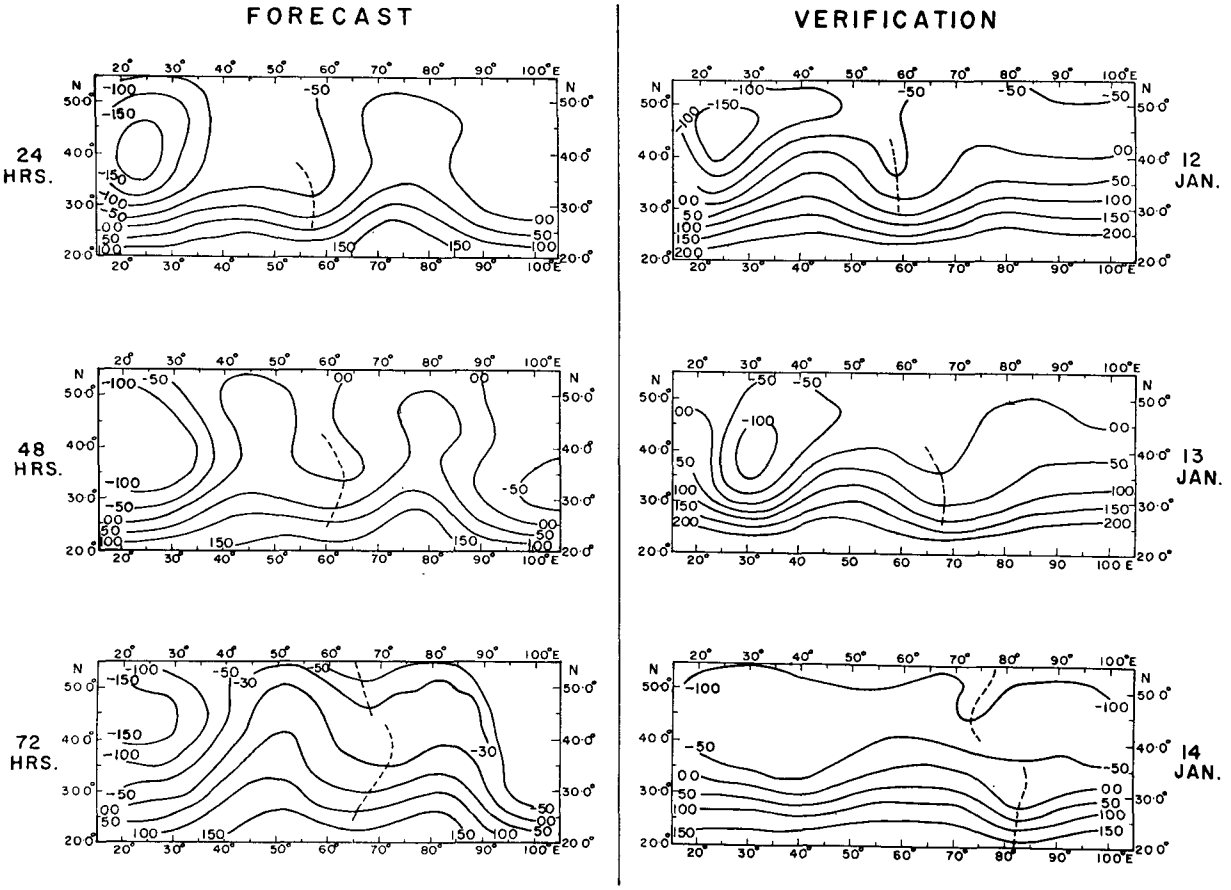

FIG. 2b. Forecast streamfunction charts at 500 mb for 24, 48, and 72 hr and corresponding verification streamfunction charts. Initial map is shown in Fig. 2a. The dashed line gives the position of the axis of the trough.

3) Forecasts using 22 December 1968 initial data have considerably larger errors than those beginning with 11 January 1969.
4) Barring the case of the 48-hr v-field forecast of 22 December 1968, the model forecast errors are definitely smaller than persistence errors in all cases.

The error statistics presented in Table 1, however, relate to the whole (u, v) field. It would be of interest to know the errors in forecasting the movement of the trough in the westerlies or western disturbances in a narrow latitudinal belt, although an accurate positioning of the trough axis may not be feasible with a 2°–5° grid. These errors are presented in Table 2 which shows the forecast and the actual verifying longitudinal positions of the trough line oriented more or less in a N-S direction in the subtropical belt, say at a mean latitude of 35N. It may be seen that the movement of the disturbances is generally in the right direction.

From the forecast position for the 24- and 48-hr predictions, it can be seen that the disturbance phase speed is generally underestimated in both cases as compared to the actual position. A feasible approach to correct this may be a further reduction of the grid size for reducing the truncation error. We do not expect the barotropic effects to persist for 72 hr and our purpose in presenting 72-hr charts is mainly to show the stability of the integrations.

Further, the forecast fields in Figs. 1 and 2 show errors in the proximity of the boundaries. This is probably due to inexact boundary conditions. It can be clearly seen in Fig. 1 where a spurious vorticity center appears on the chart at the right top corner on the eastern side and starts developing and moving west in the 24–72 hr forecast charts. This vitiates the error statistics, and one way to minimize their effect on the forecast of the movement of disturbances is to choose the grid area such that the disturbance is in the middle in the initial chart.

8. Conclusion

Forecast verification results for two situations are encouraging enough to suggest that the model may be applied generally to predict the movement of western disturbances that affect winter weather over the subtropical belt of Asia. It may also be worthwhile to apply this model to predict the movement of monsoon depressions and tropical cyclones which generally move from east to west in lower latitudes. However, for the study of these latter systems, whose wavelengths are comparatively small, a further reduction in grid size may be necessary.

TABLE 2. Verification of forecasts (degrees of longitude) of trough movement along mean latitude 35N.

Period of forecast (hr)	Forecast position	Actual position	Deviations
	Initial chart 22 December 1968 (0000 GMT)		
0	...	63.7	...
24	66.2	67.5	−1.3
48	70.0	70.0	0
72	73.7	71.2	+2.5
	Initial chart 11 January 1969 (0000 GMT)		
0	...	48.7	...
24	56.2	57.5	−1.3
48	63.7	66.2	−2.5
72	72.5	*	...

* On the actual chart, a trough appears at 72.5E along 45N; but along 35N a ridge appears instead along this longitude with a trough along 82.5E.

Acknowledgments. The authors wish to thank Mr. Lloyd Vandermann of the National Meteorological Center, NOAA, for his helpful suggestions.

They are grateful to their colleague, Mr. D. R. Sikka, for making available to them the December 1968 series of charts which he had analyzed in connection with another study. They are also indebted to Miss P. L. Kulkarni for assistance in computations.

REFERENCES

Gerrity, J. P., and R. D. McPherson, 1969: Development of a limited area fine mesh prediction model. *Mon. Wea. Rev.*, **97**, 665–669.

Hawkins, H. F., and S. L. Rosenthal, 1965: On the computation of streamfunctions from the wind field. *Mon. Wea. Rev.*, **93**, 245–252.

Krishnamurti, T. N., 1969: An experiment in numerical prediction in equatorial latitudes. *Quart. J. Roy. Meteor. Soc.*, **95**, 594–620.

Shukla, J., D. R. Sikka and K. R. Saha, 1970: Forecasting in the tropics with barotropic model with wind as input. *Preprint of Papers, Symp. Tropical Meteorology*, Hawaii, Amer. Meteor. Soc., H IV-1 to H IV-4.

Shuman, F. G. 1962: Numerical experiments with the primitive equations. *Proc. Intern. Symp. Numerical Weather Prediction*, Tokyo, Meteor. Soc. Japan, **40**, 85–107.

——, and L. W. Vandermann, 1966: Difference system and boundary conditions for the primitive-equation barotropic forecast. *Mon. Wea. Rev.*, **94**, 329–335.

Wang, H. H., and Halpern, P., 1970: Experiments with a regional fine mesh prediction model. *J. Appl. Meteor.*, **9**, 545–553.